

Ring-exchange physics in a chain of three-level ions

Sourav Biswas,¹ E. Rico,^{1,2,3,4} and Tobias Grass^{1,4}

¹*DIPC - Donostia International Physics Center,*

Paseo Manuel de Lardizábal 4, 20018 San Sebastián, Spain

²*EHU Quantum Center and Department of Physical Chemistry,*

University of the Basque Country UPV/EHU, P.O. Box 644, 48080 Bilbao, Spain

³*European Organization for Nuclear Research (CERN), Geneva 1211, Switzerland*

⁴*IKERBASQUE, Basque Foundation for Science, Plaza Euskadi 5, 48009 Bilbao, Spain*

In the presence of ring exchange interactions, bosons in a ladder-like lattice may form the bosonic analogon of a correlated metal, known as the d -wave Bose liquid (DBL). In this Letter, we show that a chain of trapped ions with three internal levels can be used to mimic a ladder-like system constrained to a maximum occupation of one boson per rung. The setup enables tunable ring exchange interactions, giving rise to a transition between a polarized regime with all bosons confined to one leg and the DBL regime. The latter state is characterized by a splitting of the peak in the momentum distribution and an oscillating pair correlation function.

Introduction. Metallic behavior is common in electronic matter: Fermionic particles partially fill an energy band. However, if matter is bosonic instead of fermionic, the particles are either expected to condense into a state with superfluid properties or to form an insulating phase [1]. The possibility of an intermediate phase in which bosonic quasiparticles exhibit metal-like behavior has long been a vivid research subject [2–4]. Bosonic lattice models that support metallic behavior have been proposed in Refs. [5, 6], with ring exchange interactions on a plaquette being the key ingredient. A quasi-one-dimensional variant of the model consists only of two chains coupled via a ring exchange term, and potentially interchain hopping [7], or extensions to multi-leg ladders [8, 9]. As a striking consequence of the ring exchange term the occurrence of an unusual strong-coupling phase of bosons has been reported, characterized by a peak splitting in the momentum distribution and sign oscillations of pair correlations, hinting towards the d -wave correlated nature of this phase which has been dubbed d -wave Bose liquid (DBL).

Realizing prototypical models in controllable quantum systems has become possible through the development of various quantum simulation platforms. Cold atoms in optical lattices have a long-standing history of being used to study many-body phases of bosons [10], and also ladder geometries have been realized with cold atoms [11], but the realization of models with ring exchange interactions remains outstanding. Bosonic lattice models have also been realized using excitons in artificial lattices [12, 13], and the dipolar nature of excitons might even provide weak ring exchange terms, but so far this platform has mostly been used to study gapped phases. Another quantum simulation platform that is very powerful for the study of one-dimensional spin models is trapped ions [14]. An XY chain of spin-1/2 degrees of freedom, $H_{XY} = \sum_{i,j} J_{ij} \sigma_i^+ \sigma_j^-$ h.c., with σ_i^\pm being raising/lowering operators of spin i , has been realized with trapped ions in Ref. [15], and is equivalent to a model

of hard-core bosons with long-range hopping $-J_{ij}$ along a chain. It has also been proposed to use the presence of nearest- and next-nearest neighbor hopping to map the chain onto a two-leg ladder [16]. Another interesting aspect of ion chains is the possibility of going beyond spin-1/2 physics by exploiting three or more internal levels. This can give rise to SU(3) physics, as proposed in Ref. [17], or spin-1 models as realized in Ref. [18], or qudit quantum computers as realized in Ref. [19].

In the present Letter, we exploit the possibility of using three-level trapped ion systems for simulating a bosonic two-leg ladder constrained to a maximum occupation of one particle per rung. Appropriately chosen Raman couplings between the levels provide, within a second-order Magnus expansion, the analogon of tunable intra-leg tunneling and ring exchange terms. We show that the tunable strength of the ring exchange term leads to a quantum phase transition into the DBL phase and that measuring pairwise correlations between the ions provides clear signatures of this transition. For weak ring exchange terms, the long-range nature of the ion systems becomes important, polarizing the system into one ladder. Our theoretical study employs the (quasi-)exact numerical methods of diagonalization (ED) and density matrix renormalization group (DMRG) through the ITensor library [20]. The DMRG algorithm [21, 22] has been an extremely reliable and effective tool for investigating different phases of matter in ladder-like systems [23–28].

Model. Let us start from the ring-exchange model on a two-leg ladder studied in Ref. [7]. Denoting by $a_{i\sigma}^\dagger$ ($a_{i\sigma}$) the creation (annihilation) operators of hard-core bosons on the sites of a ladder of length L , identified by a rung index $i \in [1, L]$ and a leg index $\sigma \in \{\downarrow, \uparrow\}$, the model reads

$$H = \sum_{i>j,\sigma} \left(-t_{ij}^\sigma a_{i\sigma}^\dagger a_{j\sigma} + K_{ij} a_{i\sigma}^\dagger a_{j\bar{\sigma}}^\dagger a_{j\bar{\sigma}} a_{i\sigma} + \text{h.c.} \right) - t_{\uparrow\downarrow} \sum_i a_{i\uparrow}^\dagger a_{i\downarrow} + \text{h.c.}, \quad (1)$$

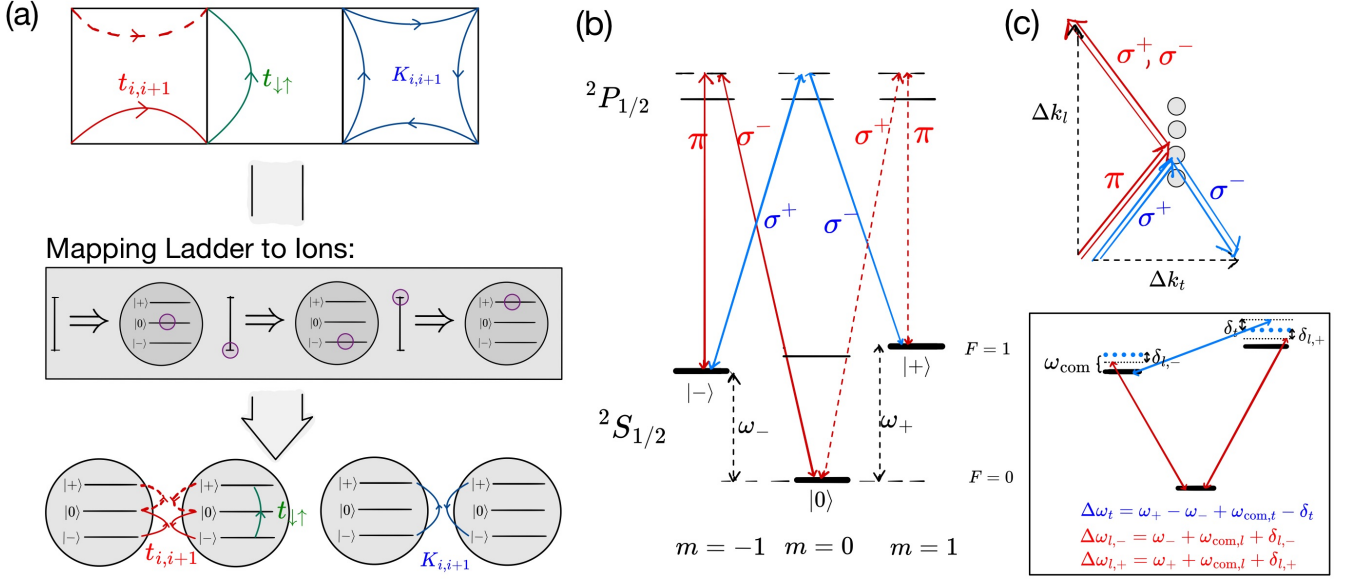


FIG. 1. (a) Mapping between the two-leg ladder and chain of three-level ions. (b,c) Implementation of intra-leg hopping and ring exchange via Raman transitions following the level diagram of $^{171}\text{Yb}^+$ shown in (b). As illustrated in (c), the pairs drawn in red couple to the longitudinal phonon direction, and are equipped with two beat notes, tuned to the τ_{-0} transition and the τ_{0+} transition, with different detunings $\delta_{l,-}$ and $\delta_{l,+}$ from the longitudinal center-of-mass mode at frequency $\omega_{\text{com},l}$, as indicated in the box. The pairs drawn in blue couple to transverse phonon modes, and are equipped with one beat-note tuned to the τ_{-+} transition with a detuning δ_t from the transversed center-of-mass mode at frequency $\omega_{\text{com},t}$. Both couplings operate on a single side-band.

where σ and $\bar{\sigma}$ denote opposite legs. In this formulation, we have accounted for a possible long-range character of intra-leg hopping t_{ij}^σ in leg σ , and ring-exchange interactions K_{ij} . In the original model of Ref. [7], these terms reduce to nearest neighbor (NN) terms, $t_{ij}^\sigma = t\delta_{j,i\pm 1}$ and $K_{ij} = K\delta_{j,i\pm 1}$, and the hopping amplitudes are equal in both legs. To map this Hamiltonian onto a chain of three-level ions, we extend the hardcore constraint from on-site to on-rung, that is, we allow for a maximum occupation of one boson per rung, $a_{i\sigma}^2 = a_{i\sigma}a_{i\bar{\sigma}} = 0$. With this constraint, the local Hilbert space on each rung is limited to three states, which we denote by $|-\rangle$ for the lower leg ($\sigma = \downarrow$) being occupied, $|+\rangle$ for the upper leg ($\sigma = \uparrow$) being occupied, and $|0\rangle$ for an empty rung. As illustrated in Fig. 1(a), the ladder can then be mapped onto a chain of three-level ions. In this formulation, intra-leg hopping and ring exchange can in principle be expressed in terms of appropriate spin-1 operator products, or more conveniently, in terms of the eight generators of the SU(3) isospin algebra [29]. As an overcomplete basis of these generators, let us introduce the SU(3) operators $\tau_{\alpha\beta}^i \equiv |i, \alpha\rangle\langle i, \beta|$, with $\alpha, \beta \in \{-, 0, +\}$ denoting the internal level of ion $i \in [1, L]$. A hopping process in the lower leg, $a_{i+1\downarrow}^\dagger a_{i\downarrow}$, is re-written as $\tau_{-,0}^{i+1} \tau_{0,-}^i$, and similarly, $a_{i+1\uparrow}^\dagger a_{i\uparrow} = \tau_{+,0}^{i+1} \tau_{0,+}^i$ for hopping in the upper leg. The ring-exchange term takes an equally simple quadratic form $a_{i\uparrow}^\dagger a_{i+1\downarrow}^\dagger a_{i+1\uparrow} a_{i\downarrow} = \tau_{+,-}^i \tau_{-,+}^{i+1}$, and inter-leg hopping takes the form of a magnetic field term,

$$a_{i\uparrow}^\dagger a_{i\downarrow} = \tau_{+,-}^i.$$

Implementation. To implement this SU(3) model with trapped ions, we start from a free ion Hamiltonian with three levels, $H_0 = \hbar\omega_-|-\rangle\langle -| + \hbar\omega_+|+\rangle\langle +|$, where the $|0\rangle$ level is chosen to be at zero energy, and $\omega_-, \omega_+ > 0$. As illustrated in Fig. 1(b), and following the implementation of spin-1 physics in Ref. [18], these three levels could be two Zeeman split levels of the $F = 1$ manifold, and the $F = 0$ level of $^2S_{1/2}$ in $^{171}\text{Yb}^+$. In this case, the frequency difference $(\omega_+ - \omega_-)$ is determined by the Zeeman splitting, and $(\omega_+ + \omega_-)/2$ is the frequency difference between $F = 0$ and $F = 1$. The desired SU(3) Hamiltonian is implemented via a Raman coupling which produces transitions between internal states, cf. Fig. 1(b), together with a phononic side-band transition, cf. Fig. 1(c), selected by the wave vector difference Δk and the beat-note of the coupling. To treat the optical coupling, we go into the rotating frame of H_0 and apply a rotating wave approximation. With this, and under the Lamb-Dicke assumption, i.e. $e^{i\Delta kx} \approx 1 + i\Delta kx$, the coupling between levels $\alpha, \beta \in \{-, 0, +\}$ can be expressed as

$$h_{\alpha\beta}(t) = \frac{i\Omega_{\alpha\beta}}{2} \sum_{i,m} \eta_{m,i} e^{i(\mu_{\alpha\beta} - \omega_m)t} b_m^\dagger \tau_{\alpha\beta}^i + \text{h.c.}, \quad (2)$$

with $\Omega_{\alpha\beta}$ being the Rabi frequency, $\eta_{m,i}$ the Lamb-Dicke parameter for mode m at ion i , and b_m^\dagger (b_m) the creation (annihilation) operator of this mode. Each coupling has an individual beat-note $\mu_{\alpha\beta} = \omega_{\text{com},\alpha\beta} + \delta_{\alpha\beta}$,

detuned by $\delta_{\alpha\beta}$ from the center-of-mass (com) mode of the selected phonon branch, with frequency $\omega_{\text{com},\alpha\beta}$. In total, we require three such coupling terms, $H(t) = h_{0-}(t) + h_{0+}(t) + h_{-+}(t)$, where h_{-0} and h_{0+} implement the hopping (red couplings in Fig. 1(b)), and h_{-+} produces the ring-exchange (blue coupling). Using the Raman laser arrangement as shown in Fig. 1(c), the coupling for the ring exchange uses transverse phonons, whereas the couplings for the hopping terms use longitudinal phonons. This choice ensures the proper signs of the effective isospin interactions, arising in second-order perturbation (see below). Specifically, coupling to transverse phonons allows for implementing antiferromagnetic interactions (hence $K > 0$), whereas coupling to longitudinal phonons allows for ferromagnetic interactions (hence $-t < 0$), both in regimes where the coupling parameters exhibit a power-law decay behavior [30, 31].

The effective Hamiltonian arises from a non-oscillatory term, $e^{-iH_{\text{eff}}t/\hbar}$, in the second-order Magnus expansion of the time-evolution operator, $\mathcal{U}(t,0) \approx \mathcal{T} \exp\{-\frac{i}{\hbar} \int_0^t d\tau_1 \int_0^{\tau_1} d\tau_2 [H(\tau_1), H(\tau_2)]/\hbar\}$. Through the choice $\delta_{-0} \neq \delta_{0+}$, it is avoided that the $|-\rangle\langle 0|$ transition interferes with the $|0\rangle\langle +|$ transition, despite both transitions using the same phonon branch. The effective Hamiltonian takes a form that is similar to an XY model:

$$H_{\text{eff}} = \sum_{i \neq j} \sum_{\alpha \neq \beta} J_{\alpha\beta}^{ij} \tau_{\alpha\beta}^i \tau_{\alpha\beta}^j + \sum_{i,\alpha} V_{\alpha} \tau_{\alpha\alpha}^i. \quad (3)$$

In the ladder picture, the second term can be interpreted as a chemical potential on the two legs. We note that V_{α} does not only depend on the involved coupling parameters (Rabi frequencies, detunings) but also on the phonon occupation numbers. Therefore, it might be hard to tune this term. However, we will concentrate on the case without inter-leg tunneling ($t_{\uparrow\downarrow} = 0$). Then, the population in each leg is conserved, and the chemical potential term becomes irrelevant. With this, we can focus on the first term in Eq. (3). This term produces the desired intra-leg hoppings as well as the ring exchange terms. The corresponding amplitudes are defined by the coupling parameters:

$$J_{\alpha\beta}^{ij} = \sum_{\mathbf{m}} \eta_{\mathbf{m},i} \eta_{\mathbf{m},j} \frac{\hbar \Omega_{\alpha\beta}^2}{\mu_{\alpha\beta} - \omega_{\mathbf{m}}}. \quad (4)$$

Despite different detunings δ_{-0} and δ_{0+} , the hopping amplitudes in both legs $t_{ij}^{\sigma} = -J_{\sigma 0}^{ij}$ can be made approximately equal via an appropriate choice of Rabi frequencies. The ring-exchange amplitude $K_{ij} = J_{-+}^{ij}$ can be tuned independently. By choosing a detuning sufficiently far away from the phonon spectrum, all parameters may decay according to a $|i-j|^{-3}$ power law, although a slower decay is experimentally more feasible. In the following, we only assume that the decay strongly suppresses long-range terms, such that we can limit ourselves to the dominant NN terms, and sub-leading next-nearest neighbor

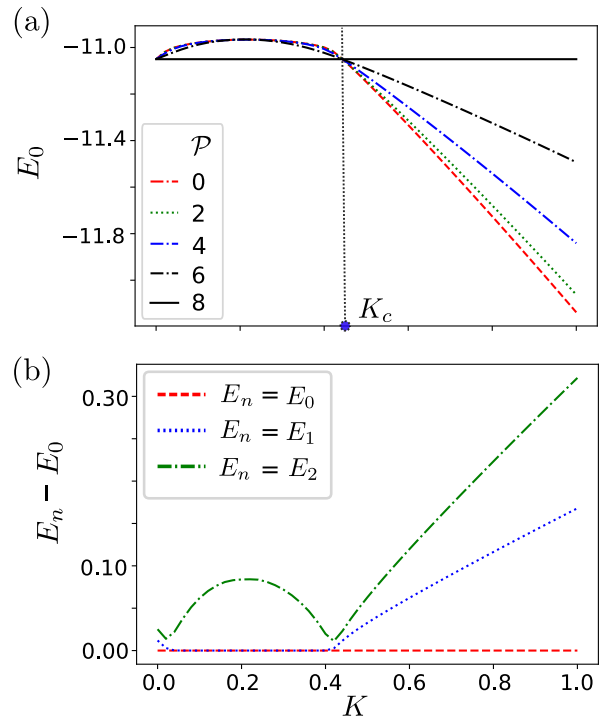


FIG. 2. Eigen-energies, computed using ED (for $L = 16$), are shown as a function of K . (a) depicts the lowest energies for various polarization sectors. (b) shows the energy difference between different lowest-lying energies in $\mathcal{P}=0$.

(NNN) terms. In terms of the original model Eq. (1), this means that from now on the only non-zero terms will be NN and NNN hopping $t_{i,i+1}^{\sigma} \equiv t$ and $t_{i,i+2} = t_2$, as well as non-zero NN and NNN ring exchange $K_{i,i+1} \equiv K$ and $K_{i,i+2} = K_2$. For concreteness, we concentrate on the choice $t_2/t = K_2/K = 0.2$ and set $t = 1$.

Results. To study the model numerically via ED and DMRG¹, we fix the filling $n_f = (\mathcal{N}_+ + \mathcal{N}_-)/(2L) = \sum_i \langle (S_z^i)^2 \rangle / (2L)$ to 1/4, as well as the polarization $\mathcal{P} = \mathcal{N}_+ - \mathcal{N}_- = \sum_i \langle S_z^i \rangle$. In these definitions, \mathcal{N}_{\pm} refers to the number of particles in the $|\pm\rangle$ legs, mapped onto the internal state of the ions via the spin-1 notation, $S_z^i = \tau_{++}^i - \tau_{--}^i$. The lowest energy in each polarization sector is plotted in Fig. (2)(a) as a function of K . For $K < K_c \approx 0.44$, the true ground state is fully polarized ($|\mathcal{P}| = 2Ln_f$). In this configuration, one leg remains empty, and hence, no ring exchange can occur, and the energy does not depend on K . Interestingly, the lowest energy states in the other polarization sectors are all (at least approximately) degenerate. The nature of these states can be understood from Fig. 3, where we complete

¹ The DMRG sweeps are performed with the maximum allowed bond dimension varying between 1000-5000, depending upon the requirement, and truncation error is kept at 10^{-10} .

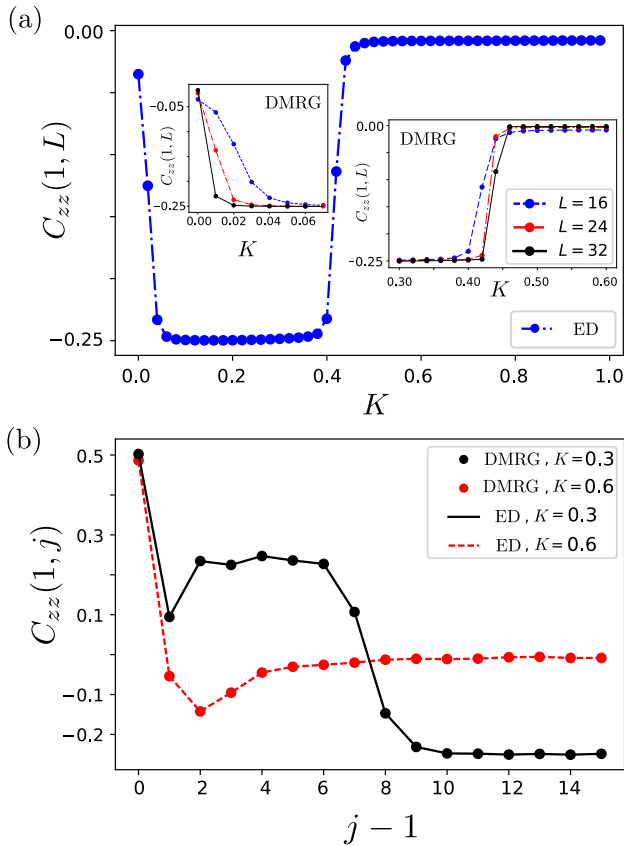


FIG. 3. (a) The correlation $C_{zz}(1, L)$ is plotted as a function of K using ED ($L = 16$) at $\mathcal{P} = 0$. The system passes from an ordered phase to a phase without long-range order. This transition persists with varying L , as observed from DMRG (in the insets). (b) The correlator $C_{zz}(1, j)$ behaves differently in these two phases (i.e. $K < K_c$ and $K > K_c$).

ment the results from ED with that of DMRG, showing the correlation function $C_{zz}(i, j) = \langle S_z^i S_z^j \rangle$ of the lowest energy state in the fully unpolarized sector $\mathcal{P}=0$. Here, we concentrate on this sector, as the true ground state resides in $\mathcal{P}=0$ for $K > K_c$, as discussed later. The solid line in Fig. 3(b) shows that there is a domain wall, with the left half of the system being polarized in one leg, and the right half being polarized in the other leg. We associate the energy gap to the fully polarized with the energy cost of such a domain wall. The domain-wall picture also provides an intuitive explanation for the double degeneracy of this state, seen in Fig. (2)(b). We note that the domain-wall picture does not apply for very small values of K , as seen in Fig. 3(a). In this regime, the quasi-degeneracy of many states leads to different behavior, but data in the inset suggest that the critical K of this regime tends to zero when the system size is increased.

The lowest-energy state becomes the unique true ground state for $K > K_c$. The level crossing between lowest-energy states in different polarization sectors co-

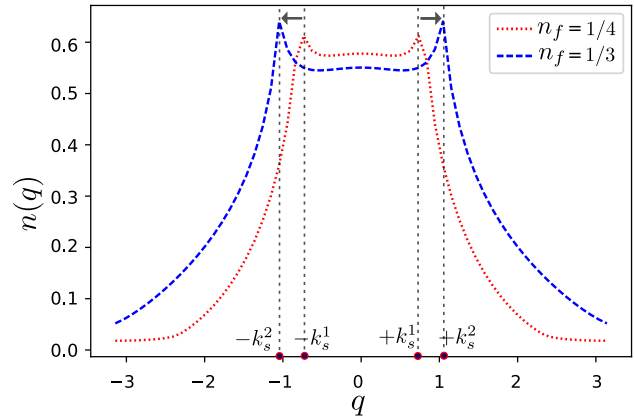


FIG. 4. $n(q)$ is plotted for $K = 0.6$, using DMRG for $L = 60$. The absence of zero momenta peak and the presence of peaks at $k_s = \pi n_f$ are also consistent with the known features of such a phase. We see that changing n_f from $1/4$ to $1/3$ shifts the peaks.

incides with an avoided level crossing within the polarized sector, see Fig. (2)(b). Therefore, even if the polarization is fixed to $\mathcal{P}=0$, as done in Fig. (3), an abrupt change of correlations can be observed at $K > K_c$ phase. Specifically, we note that the long-range order present at small K is lost, as indicated by $C_{zz}(1, j) \rightarrow 0$ for large j .

Importantly, the ground state for $K > K_c$ carries clear signatures of a d -wave Bose liquid (DBL). Two quantities of utmost interest in defining the DBL phase are: (i) the momentum distribution function $n(q) = \sum_{j_1, j_2} \sum_{\sigma=\uparrow, \downarrow} \exp(-iq(j_1 - j_2)) \langle a_{j_1, \sigma}^\dagger a_{j_2, \sigma} \rangle / L$, and (ii) the pair correlation between diagonal sites of the two-leg ladder, given by $P_2(\Delta x) = \langle a_{1, \uparrow}^\dagger a_{2, \downarrow}^\dagger a_{\Delta x + \gamma, \uparrow} a_{\Delta x + \eta, \downarrow} \rangle$. The choice ($\gamma = 1, \eta = 2$) denotes correlation between two parallel diagonals and ($\gamma = 2, \eta = 1$) implies correlation between two perpendicular diagonals. The convention is schematically described in the appendix.

In Fig. (4), the momentum distribution $n(q)$ is plotted for a relatively large system at $K = 0.6 > K_c$. We note the absence of a zero momentum peak, which indicates a lack of long-range order. The $P_2(\Delta x)$ are shown in the appendix. We note that the oscillation in $P_2(\Delta x)$ and the position of the $n(q)$ peaks, both are connected to the filling of the ladder, as has already been worked out in Ref. [7]. As another indicator of the liquid-like behavior of the system for $K > K_c$, we have also studied the z -component of spin structure factor defined as, $\mathcal{S}_z(q) = \sum_{j_1, j_2} \exp(-iq(j_1 - j_2)) \langle S_z^{j_1} S_z^{j_2} \rangle / L$, which has sharp peaks for $K < K_c$, but gets smoothed for $K > K_c$. Corresponding data is shown in the appendix.

Discussion and Outlook. In this Letter, we have proposed to use a chain of three-level ions to implement a model of bosons on a two-leg ladder with hard-core conditions on each rung. The setup allows us to explore the effect of tunable ring exchange interactions K , and we

have shown that they produce a transition from a polarizing regime at small K to a regime with features of a d -wave Bose liquid at larger K .

The recent advancements in trapped ion experiments [32] present themselves as an ideal platform for realizing the physics under study. However, we note that trapped ion systems feature all-to-all couplings, whereas our study has focused on a model with only nearest- and next-to-nearest neighbor couplings, to facilitate DMRG calculations. Using ED, we have explicitly checked that the reported behavior qualitatively persists also in the presence of all-to-all interactions, as long as they decay with a power-law exponent of two or larger. Such a decay can easily be achieved when the coupling is transmitted by transverse phonons, as used here to implement the ring exchange term, however, it might be hard to achieve with longitudinal phonons, due to a larger bandwidth of the spectrum [31]. Since we rely on longitudinal phonons in order to implement the hopping terms through anti-ferromagnetic couplings, additional tuning might be necessary to achieve sufficiently fast decay. One possibility here is Floquet engineering techniques, see for instance Ref. [33, 34]. A flexible alternative to the analog implementation of the model is the simulation using a digital qutrit quantum computer [19].

Finally, let us also comment on the possibility of implementing the hopping term via ferromagnetic interactions transmitted through transverse phonons. The negative sign of the hopping amplitude amounts to a π -flux which, quite interestingly, is found to stabilize the DBL regime even in the absence of ring exchange. Although such a setup is experimentally less demanding, in this paper we have focused on the implementation with $t > 0$ which features a DBL transition induced via ring exchange interactions.

Acknowledgments. The authors thank Martin Ringbauer and Claire Edmunds for reading our manuscript and for providing helpful feedback on experimental aspects and implementation. We acknowledge the financial support received from the IKUR Strategy under the collaboration agreement between the Ikerbasque Foundation and DIPC on behalf of the Department of Education of the Basque Government. T.G. acknowledges funding by the Department of Education of the Basque Government through the project PIBA_2023_1.0021 (TENINT), and by the Agencia Estatal de Investigación (AEI) through Proyectos de Generación de Conocimiento PID2022-142308NA-I00 (EXQUSMI). This work has been produced with the support of a 2023 Leonardo Grant for Researchers in Physics, BBVA Foundation. The BBVA Foundation is not responsible for the opinions, comments, and contents included in the project and/or the results derived therefrom, which are the total and absolute responsibility of the authors. E.R. acknowledges support from the BasQ strategy of the Department of Science, Universities, and Innovation of

the Basque Government. E.R. is supported by the grant PID2021-126273NB-I00 funded by MCIN/AEI/10.13039/501100011033 and by “ERDF A way of making Europe” and the Basque Government through Grant No. IT1470-22. This work was supported by the EU via QuantERA project T-NiSQ grant PCI2022-132984 funded by MCIN/AEI/10.13039/501100011033 and by the European Union “NextGenerationEU”/PRTR. This work has been financially supported by the Ministry of Economic Affairs and Digital Transformation of the Spanish Government through the QUANTUM ENIA project called – Quantum Spain project, and by the European Union through the Recovery, Transformation, and Resilience Plan – NextGenerationEU within the framework of the Digital Spain 2026 Agenda.

END MATTERS

Modulation in P_2

We study the pair correlation at different filling factors. The D-wave nature of the DBL is captured by this correlation. The results are shown below:

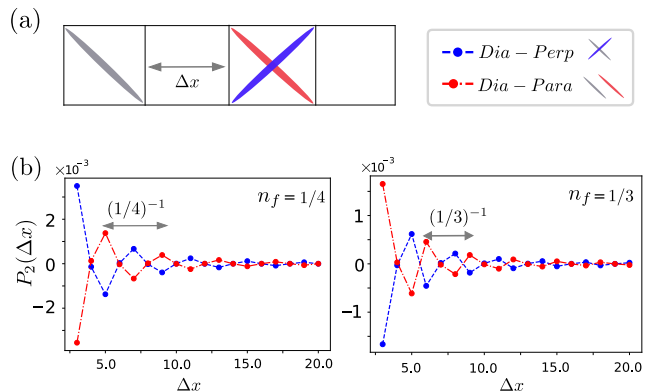


FIG. 5. The $P_2(\Delta x)$ for parallel diagonals: *Dia – Para* ($\gamma = 1, \eta = 2$) and perpendicular diagonals: *Dia – Perp* ($\gamma = 2, \eta = 1$) are opposite in sign and oscillate with a period $1/n_f$. In (a) we show the convention used for calculating the pair correlation and in (b) results for different fillings are depicted. We observe changing n_f changes the modulation in P_2 which is consistent with the shifting of peaks in FIG. (4).

Structure factor

We see from FIG. (3), that for $K < K_c$ the correlation $C_{zz}(1, j)$ changes sign at $L/2$, signifying the existence of two regions with different polarizations. The length of such domains is $L/2$, which is consistent with the appearance of sharp peaks in \mathcal{S}_z at wave vector $q = 2\pi/(L/2)$, as shown in FIG. (6). In the inset of the

same figure, one can find out how no such peak exists in $K > K_c$.

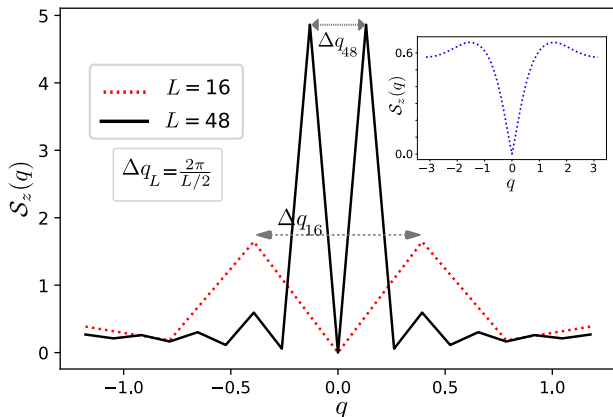


FIG. 6. $S_z(q)$ computed using DMRG. At $K = 0.3$, a comparison between $L = 16, 48$ shows the persistence of sharp peaks with Δq_L wave vector. In the inset, we see data for $L = 48$ at $K = 0.6$. The smoothness of S_z suggests an absence of any true long-range order. This is a characteristic of the DBL phase.

[1] M. P. A. Fisher, P. B. Weichman, G. Grinstein, and D. S. Fisher, Boson localization and the superfluid-insulator transition, *Phys. Rev. B* **40**, 546 (1989).

[2] P. Phillips and D. Dalidovich, The elusive bose metal, *Science* **302**, 243 (2003).

[3] C. Yang, Y. Liu, Y. Wang, L. Feng, Q. He, J. Sun, Y. Tang, C. Wu, J. Xiong, W. Zhang, X. Lin, H. Yao, H. Liu, G. Fernandes, J. Xu, J. M. Valles, J. Wang, and Y. Li, Intermediate bosonic metallic state in the superconductor-insulator transition, *Science* **366**, 1505 (2019).

[4] A. Hegg, J. Hou, and W. Ku, Geometric frustration produces long-sought bose metal phase of quantum matter, *Proceedings of the National Academy of Sciences* **118**, e2100545118 (2021).

[5] A. Paramekanti, L. Balents, and M. P. A. Fisher, Ring exchange, the exciton bose liquid, and bosonization in two dimensions, *Phys. Rev. B* **66**, 054526 (2002).

[6] O. I. Motrunich and M. P. A. Fisher, d -wave correlated critical bose liquids in two dimensions, *Phys. Rev. B* **75**, 235116 (2007).

[7] D. N. Sheng, O. I. Motrunich, S. Trebst, E. Gull, and M. P. A. Fisher, Strong-coupling phases of frustrated bosons on a two-leg ladder with ring exchange, *Phys. Rev. B* **78**, 054520 (2008).

[8] R. V. Mishmash, M. S. Block, R. K. Kaul, D. N. Sheng, O. I. Motrunich, and M. P. A. Fisher, Bose metals and insulators on multileg ladders with ring exchange, *Phys. Rev. B* **84**, 245127 (2011).

[9] M. S. Block, R. V. Mishmash, R. K. Kaul, D. N. Sheng, O. I. Motrunich, and M. P. A. Fisher, Exotic gapless mott insulators of bosons on multileg ladders, *Phys. Rev. Lett.* **106**, 046402 (2011).

[10] M. Greiner, O. Mandel, T. Esslinger, T. W. Hänsch, and I. Bloch, Quantum phase transition from a superfluid to a mott insulator in a gas of ultracold atoms, *Nature* **415**, 39 (2002).

[11] M. Atala, M. Aidelsburger, M. Lohse, J. T. Barreiro, B. Paredes, and I. Bloch, Observation of chiral currents with ultracold atoms in bosonic ladders, *Nature Physics* **10**, 588 (2014).

[12] C. Lagoni, S. Suffit, K. Baldwin, L. Pfeiffer, and F. Dubin, Mott insulator of strongly interacting two-dimensional semiconductor excitons, *Nature Physics* **18**, 149 (2022).

[13] C. Lagoni, U. Bhattacharya, T. Grass, R. W. Chhajlany, T. Salamon, K. Baldwin, L. Pfeiffer, M. Lewenstein, M. Holzmann, and F. Dubin, Extended bose-hubbard model with dipolar excitons, *Nature* **609**, 485 (2022).

[14] C. Monroe, W. C. Campbell, L.-M. Duan, Z.-X. Gong, A. V. Gorshkov, P. W. Hess, R. Islam, K. Kim, N. M. Linke, G. Pagano, P. Richerme, C. Senko, and N. Y. Yao, Programmable quantum simulations of spin systems with trapped ions, *Rev. Mod. Phys.* **93**, 025001 (2021).

[15] P. Jurcevic, B. P. Lanyon, P. Hauke, C. Hempel, P. Zoller, R. Blatt, and C. F. Roos, Quasiparticle engineering and entanglement propagation in a quantum many-body system, *Nature* **511**, 202 (2014).

[16] T. Graß, C. Muschik, A. Celi, R. W. Chhajlany, and M. Lewenstein, Synthetic magnetic fluxes and topological order in one-dimensional spin systems, *Phys. Rev. A* **91**, 063612 (2015).

[17] T. Graß, B. Juliá-Díaz, M. Kuś, and M. Lewenstein, Quantum chaos in $su(3)$ models with trapped ions, *Phys. Rev. Lett.* **111**, 090404 (2013).

[18] C. Senko, P. Richerme, J. Smith, A. Lee, I. Cohen, A. Retzker, and C. Monroe, Realization of a quantum integer-spin chain with controllable interactions, *Phys. Rev. X* **5**, 021026 (2015).

[19] M. Ringbauer, M. Meth, L. Postler, R. Stricker, R. Blatt, P. Schindler, and T. Monz, A universal qudit quantum processor with trapped ions, *Nature Physics* **18**, 1053 (2022).

[20] M. Fishman, S. R. White, and E. M. Stoudenmire, The ITensor Software Library for Tensor Network Calculations, *SciPost Phys. Codebases*, 4 (2022).

[21] S. R. White, Density matrix formulation for quantum renormalization groups, *Phys. Rev. Lett.* **69**, 2863 (1992).

[22] U. Schollwöck, The density-matrix renormalization group in the age of matrix product states, *Annals of Physics* **326**, 96 (2011), january 2011 Special Issue.

[23] A. Dhar, M. Maji, T. Mishra, R. V. Pai, S. Mukerjee, and A. Paramekanti, Bose-hubbard model in a strong effective magnetic field: Emergence of a chiral mott insulator ground state, *Phys. Rev. A* **85**, 041602 (2012).

[24] T. Mishra, R. V. Pai, S. Mukerjee, and A. Paramekanti, Quantum phases and phase transitions of frustrated hard-core bosons on a triangular ladder, *Phys. Rev. B* **87**, 174504 (2013).

[25] T. Mishra, R. V. Pai, and S. Mukerjee, Supersolid in a one-dimensional model of hard-core bosons, *Phys. Rev. A* **89**, 013615 (2014).

- [26] Z. Bacciconi, G. M. Andolina, T. Chanda, G. Chiriacò, M. Schirò, and M. Dalmonte, First-order photon condensation in magnetic cavities: A two-leg ladder model, *SciPost Phys.* **15**, 113 (2023).
- [27] C.-M. Halati and T. Giamarchi, Bose-hubbard triangular ladder in an artificial gauge field, *Phys. Rev. Res.* **5**, 013126 (2023).
- [28] L. Barbiero, J. Cabedo, M. Lewenstein, L. Tarruell, and A. Celi, Frustrated magnets without geometrical frustration in bosonic flux ladders, *Phys. Rev. Res.* **5**, L042008 (2023).
- [29] M. Gell-Mann, Symmetries of baryons and mesons, *Phys. Rev.* **125**, 1067 (1962).
- [30] D. Porras and J. I. Cirac, Effective quantum spin systems with trapped ions, *Phys. Rev. Lett.* **92**, 207901 (2004).
- [31] S.-L. Zhu, C. Monroe, and L.-M. Duan, Trapped ion quantum computation with transverse phonon modes, *Phys. Rev. Lett.* **97**, 050505 (2006).
- [32] C. Monroe, W. C. Campbell, L.-M. Duan, Z.-X. Gong, A. V. Gorshkov, P. W. Hess, R. Islam, K. Kim, N. M. Linke, G. Pagano, P. Richerme, C. Senko, and N. Y. Yao, Programmable quantum simulations of spin systems with trapped ions, *Rev. Mod. Phys.* **93**, 025001 (2021).
- [33] F. Kranzl, S. Birnkammer, M. K. Joshi, A. Bastianello, R. Blatt, M. Knap, and C. F. Roos, Observation of magnon bound states in the long-range, anisotropic heisenberg model, *Phys. Rev. X* **13**, 031017 (2023).
- [34] N. Kotibhaskar, C.-Y. Shih, S. Motlakunta, A. Vogliano, L. Hahn, Y.-T. Chen, and R. Islam, Programmable xy-type couplings through parallel spin-dependent forces on the same trapped ion motional modes, *Phys. Rev. Res.* **6**, 033038 (2024).